

Online supplementary material for “Towards a “glocalised” management of tuna based on causation between the stock and its component belonging the local EEZs: The case of yellowfin tuna in the Eastern Atlantic and its local resource in the Ivorian EEZ”

Akia S., Amandé M. and Gaertner D.

03/11/2022

VAST models framework:

```
FieldConfig = c("Omega1"=1, "Epsilon1"=1, "Omega2"=1, "Epsilon2"=1)
RhoConfig = c("Beta1"=3, "Beta2"=3, "Epsilon1"=4, "Epsilon2"=4)
OverdispersionConfig = c(1,1)
ObsModel = c(2,1)
```

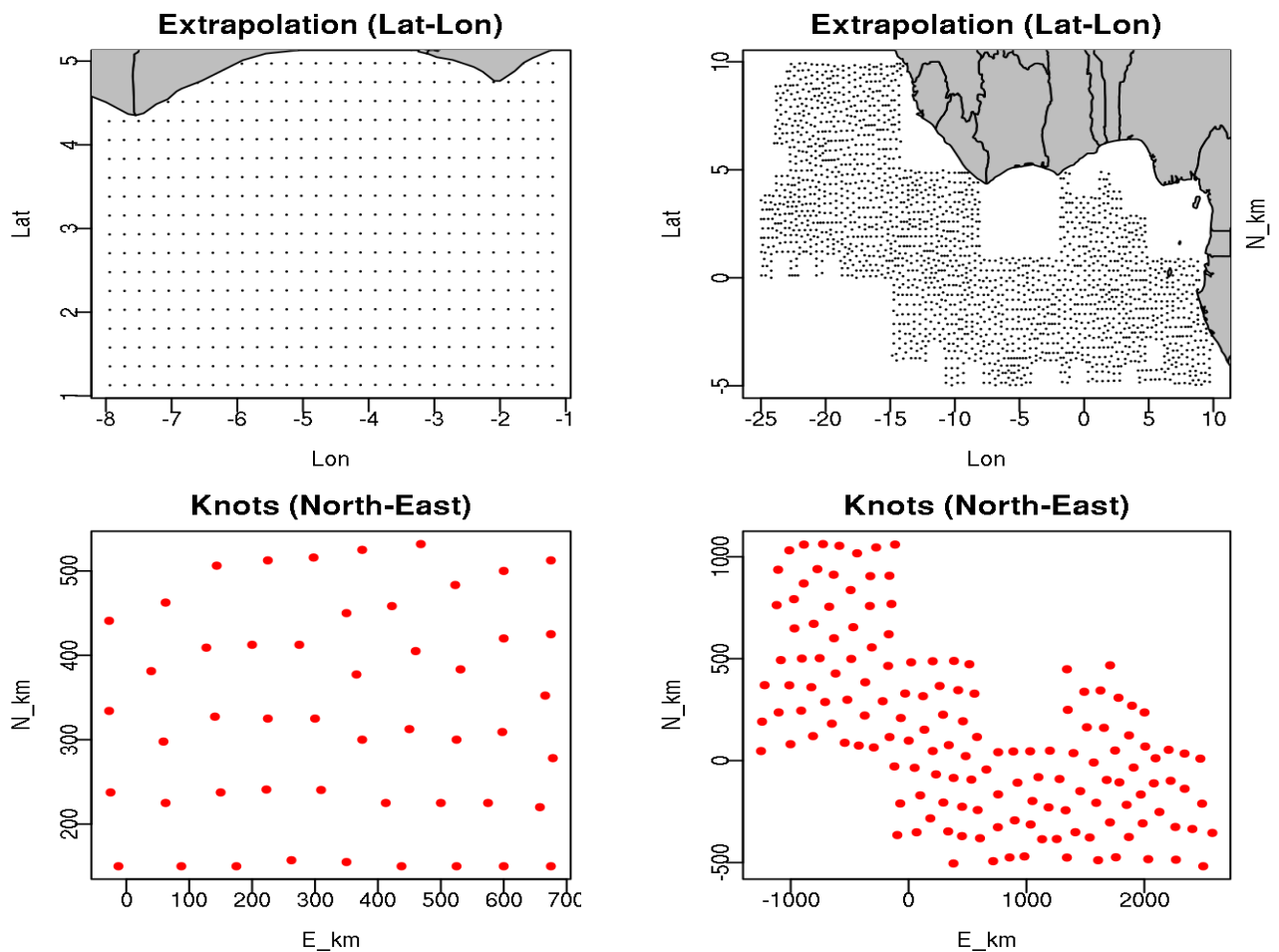


Fig. S1: Visualisation of the spatial structure used to approximate the spatial variation in each case-study (after projecting Latitude/Longitude to UTM coordinates measured in eastings (x-axis) and northings (y-axis). Red circles show the location of interior knots (50 for the local zone and 150 for the global zone) where this dots was chosen a priori and knots were then allocated using a k-means algorithm in proportion to the available sampling data. Black dots represent the extrapolation-grid ($\approx 0.227^\circ$ for local zone and $\approx 0.45^\circ$ for the global zone) used when approximating the integral across the fishing location.

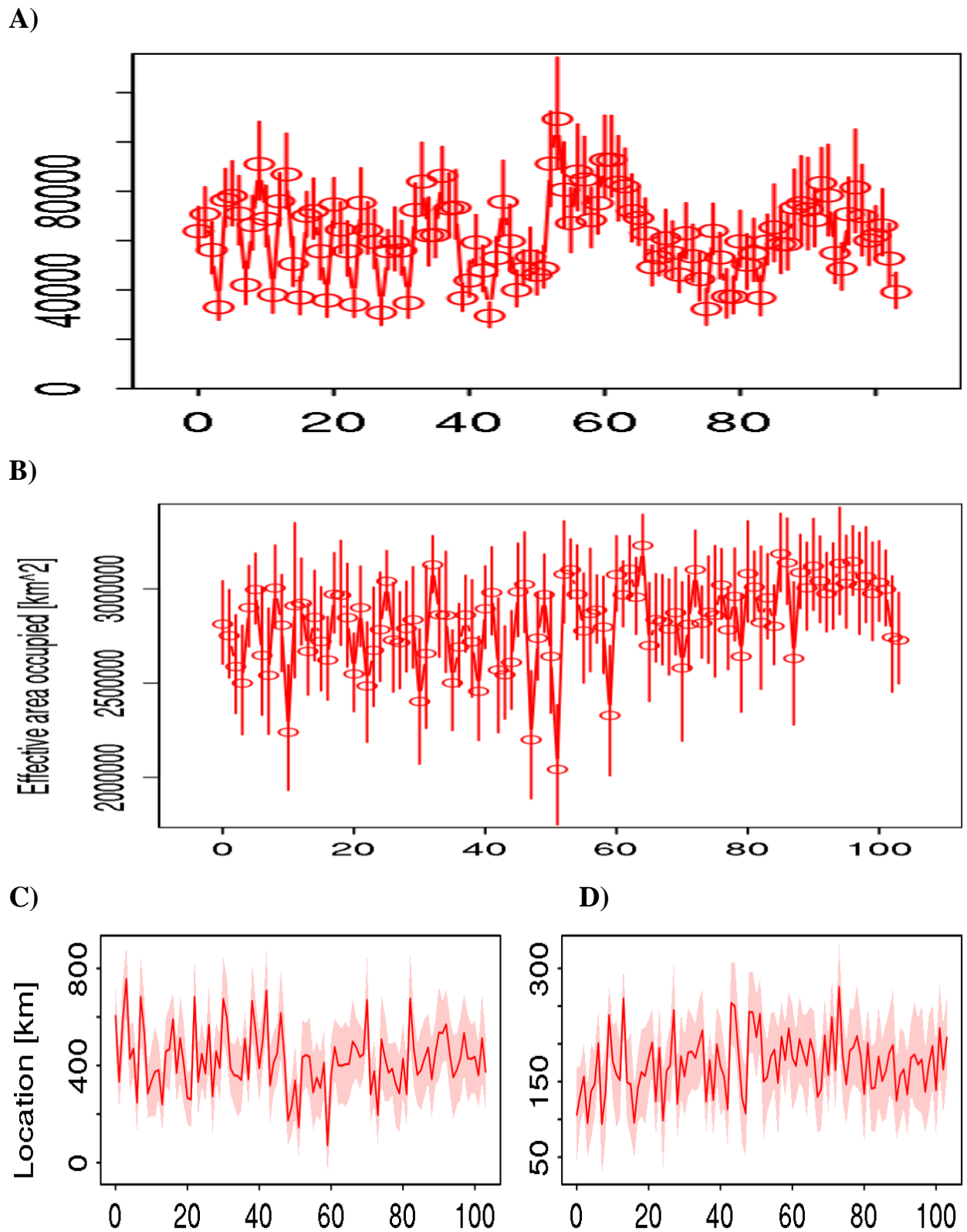
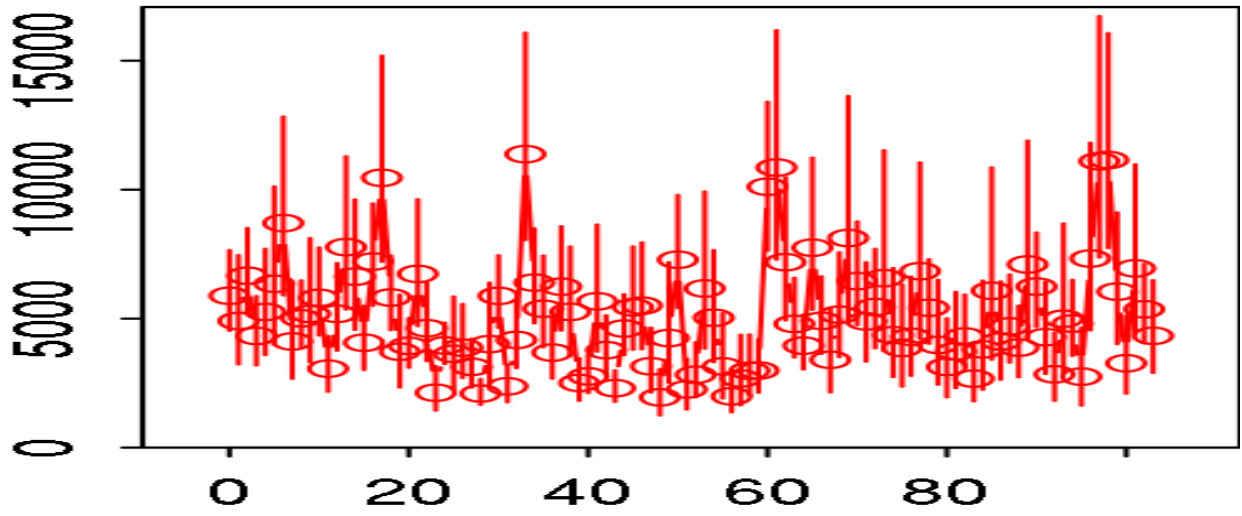
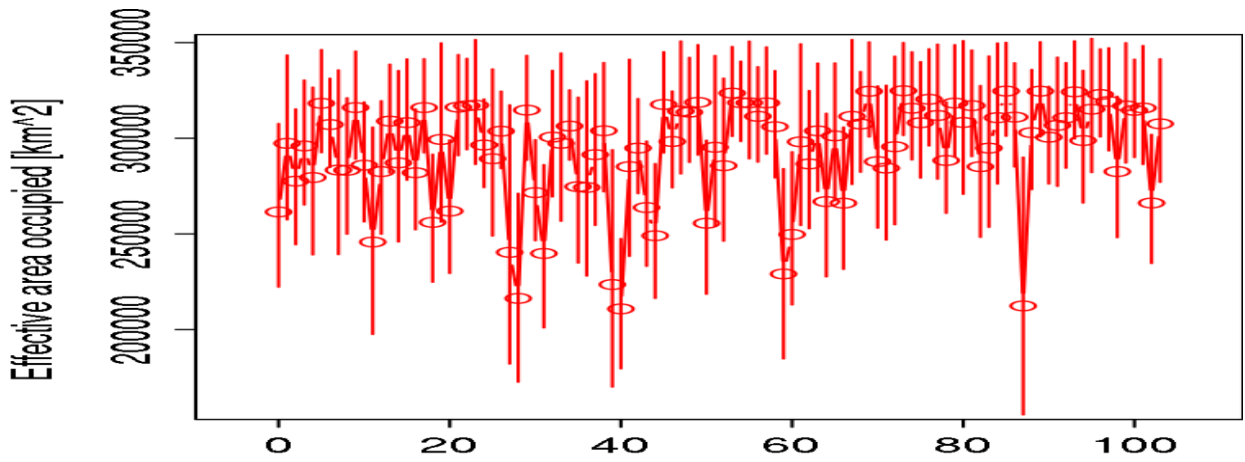


Fig. S2: Abundance indices (A; representing total biomass at the chosen spatial domain, in metric tons), effective area occupied (B; representing area needed to contain the population at average biomass-density, in km²), and northward (C) - eastward (D) center-of-gravity (C and D; representing the centroid of the population) each showing bias-corrected maximum likelihood estimate (ovals) and +/- one standard error (whisker) for each quarterly index of the adult yellowfin tuna resource in the global area; the period is from 1993 to 2018 (26 years * 4 = 104 quarters).

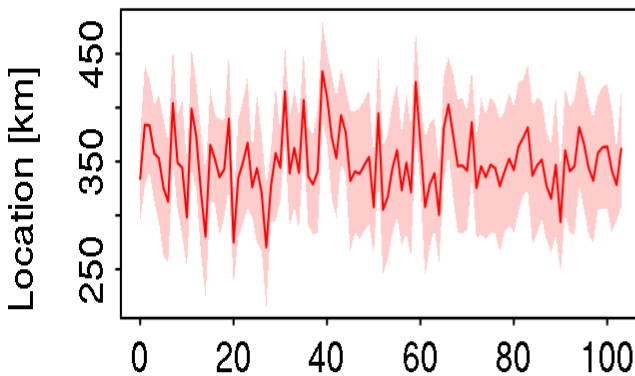
A)



B)



C)



D)

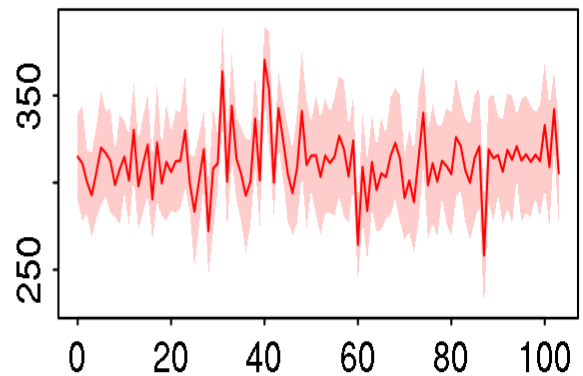


Fig. S3: Abundance indices (A; representing total biomass at the chosen spatial domain, in metric tonnes), effective area occupied (B; representing area needed to contain the population at average biomass-density, in km²), and northward (C) - eastward (D) center-of-gravity (C and D; representing centroid of the population) each showing bias-corrected maximum likelihood estimate (ovals) and +/- one standard error (whisker) for each quarterly index of the adult yellowfin tuna resource in the EEZ of Côte d'Ivoire; the period is from 1993 to 2018 (26 years *4 =104 quarters).

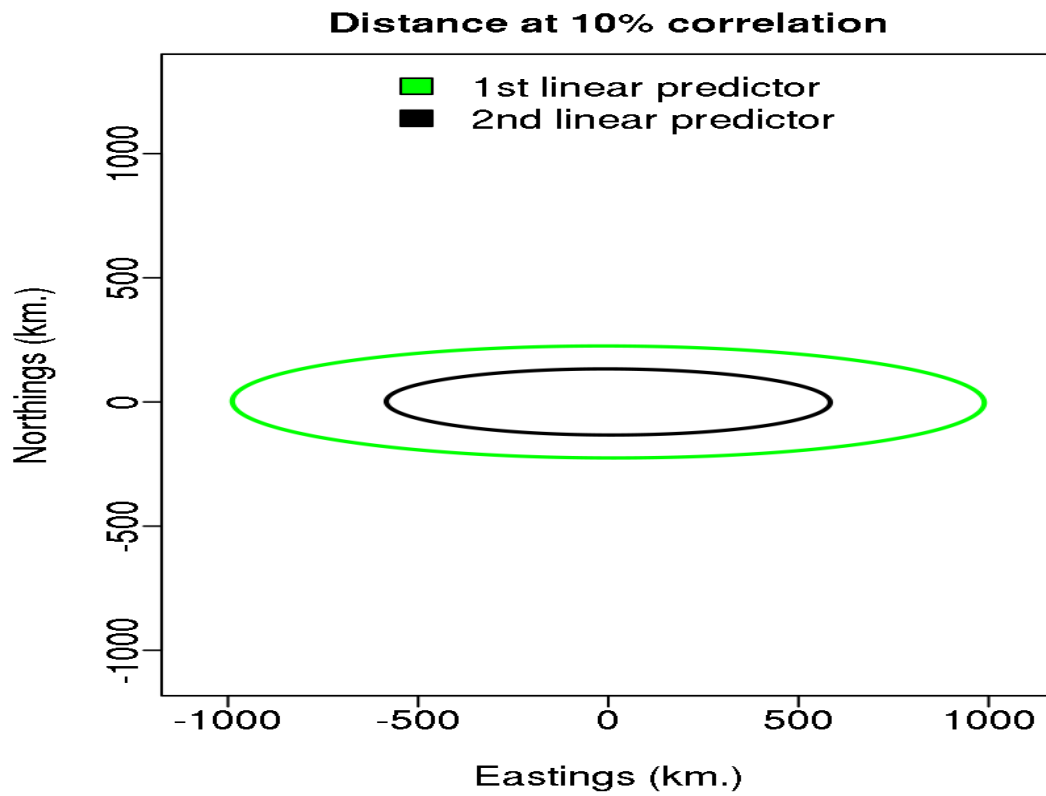


Fig. S4: The predicted geometric anisotropy for the GLOBAL model. The ellipses give the 10% decorrelation distance for each of the two model components (delta model).

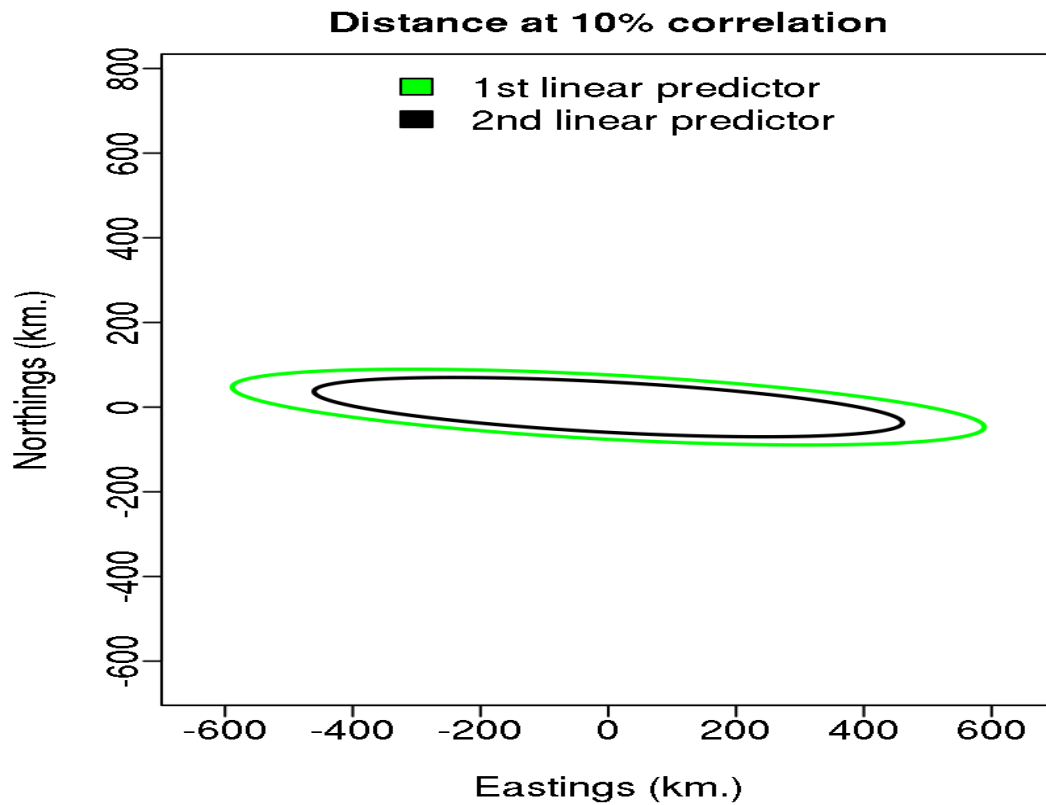
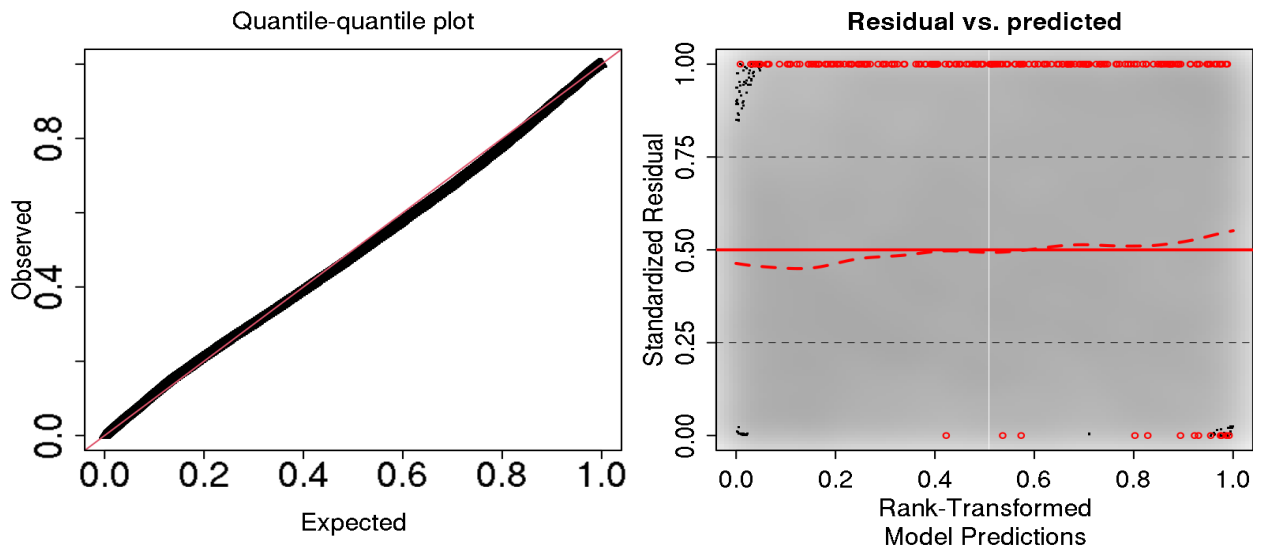


Fig. S5: The predicted geometric anisotropy for the LOCAL model. The ellipses give the 10% decorrelation distance for each of the two model components (delta model).

A)

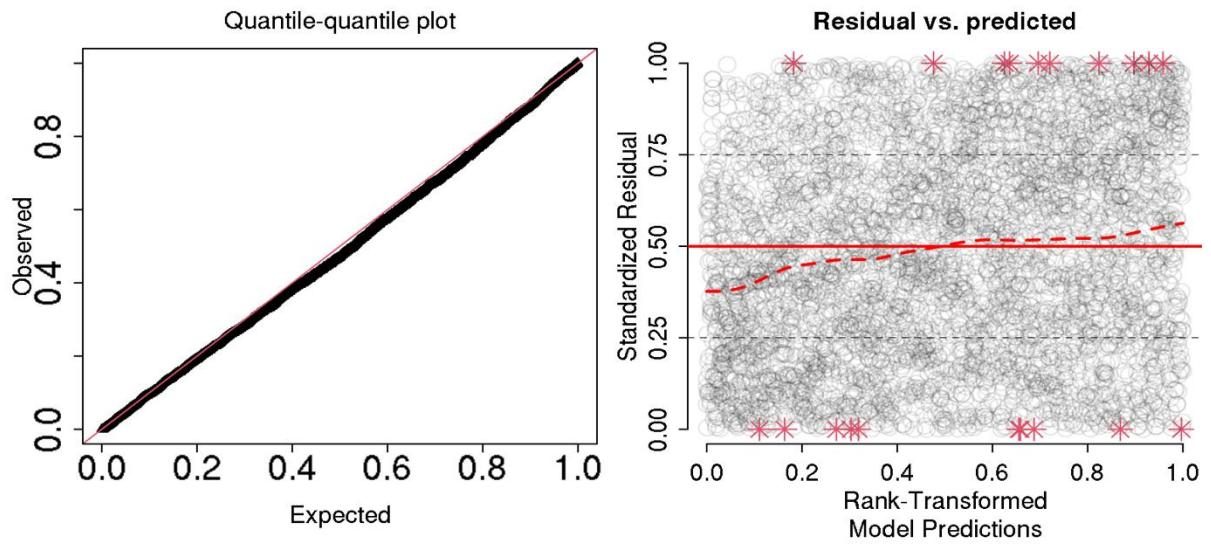


B)



Fig. S6:A)The quantile-quantile plot of residuals (left) and plot of how residuals vary with magnitude of the prediction (right). B) Spatial map of quantile residuals by quarter. Results for the GLOBAL area.

A)



B)

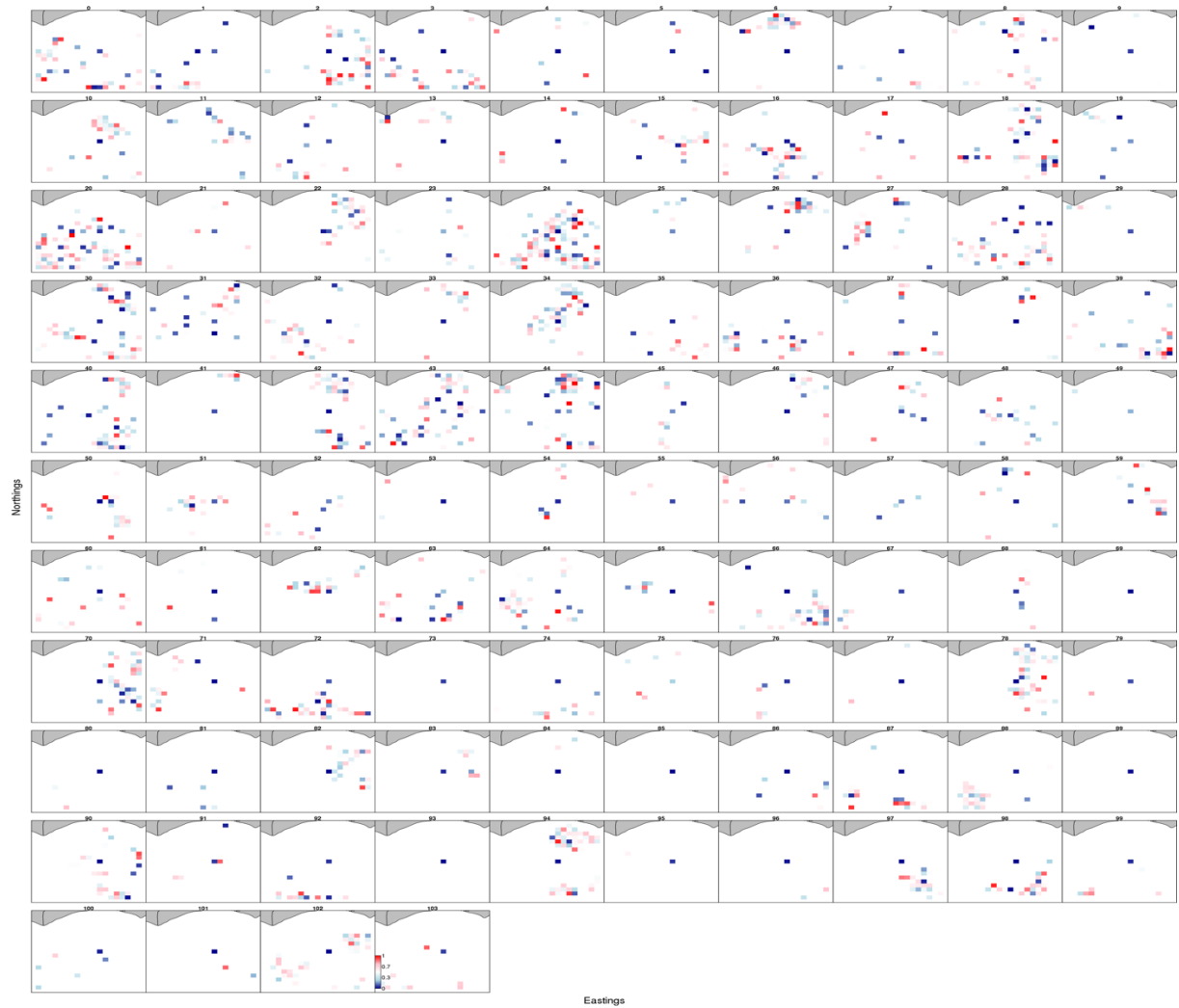


Fig. S7:A) The quantile-quantile plot of residuals (left) and plot of how residuals vary with the magnitude of the prediction (right). B) Spatial map of quantile residuals per quarter. Results for the LOCAL area.

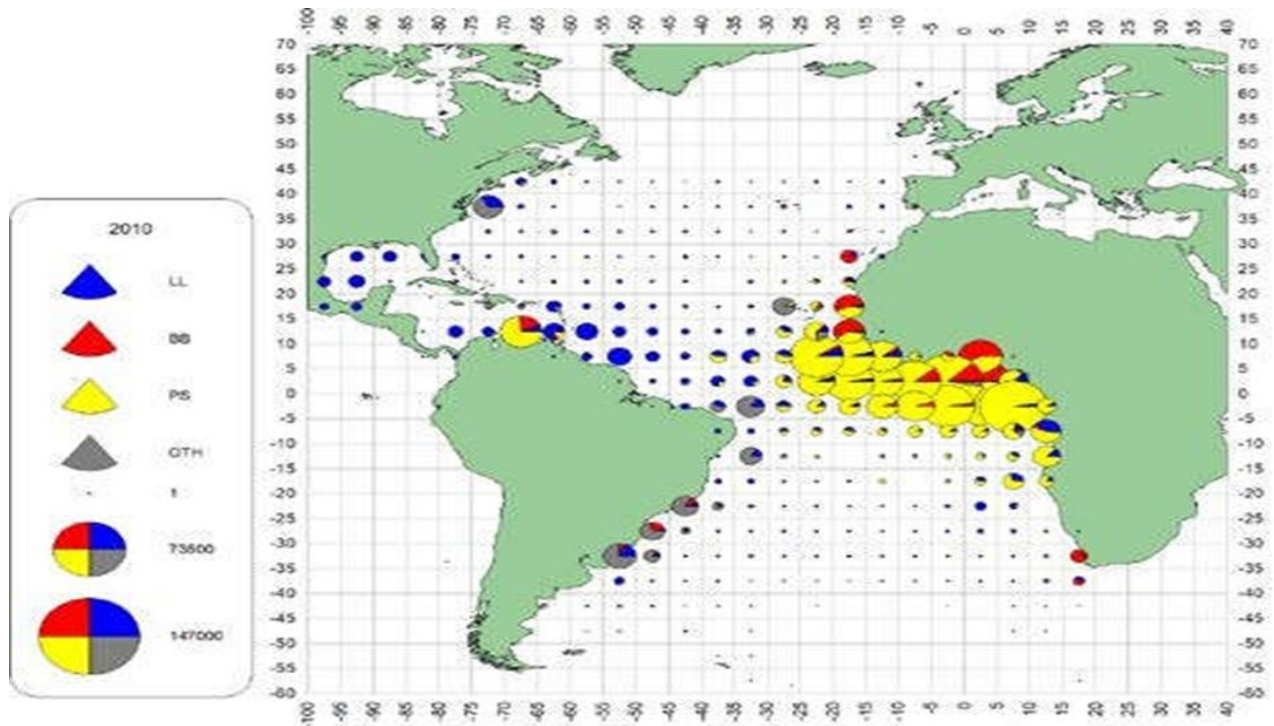


Fig. S8: Geographical distribution of yellowfin tuna total catches by major gears in the Atlantic Ocean (ICCAT zone) from 2010 to 2016 (Source: ICCAT, 2019).

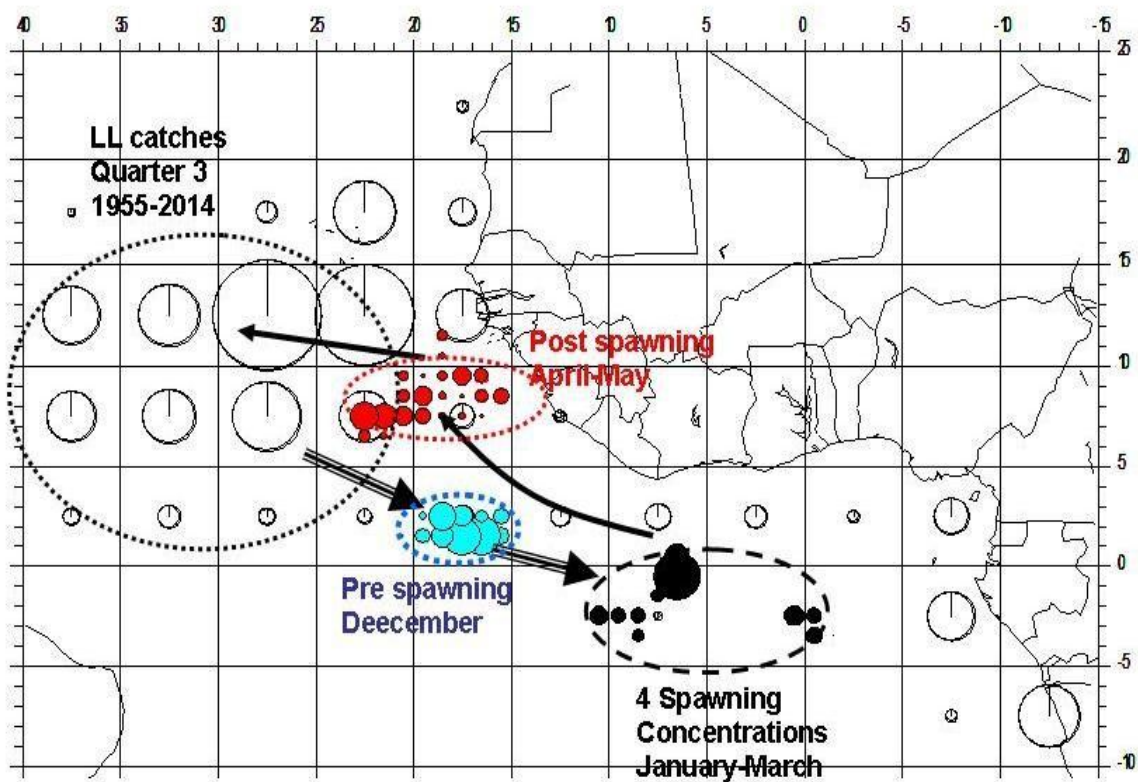
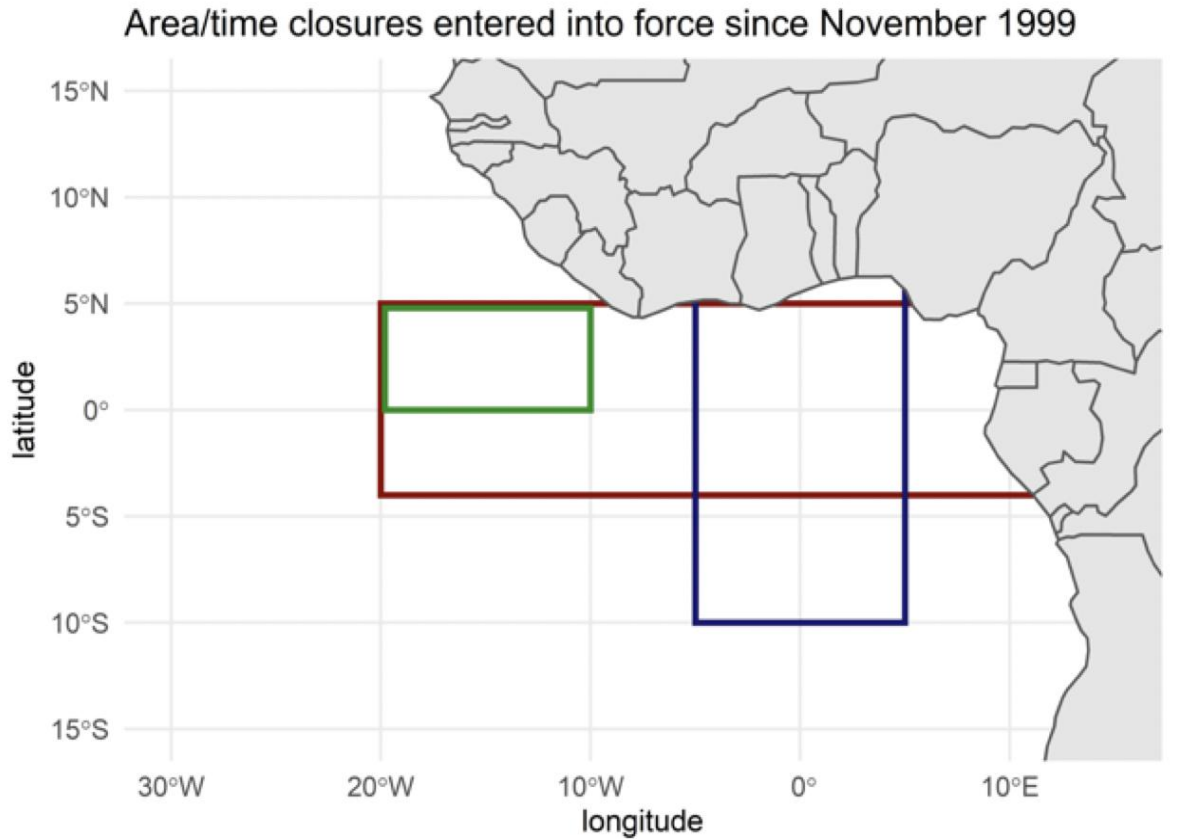


Fig. S9: Overview of a hypothetical spawning migration pattern of adult yellowfin, from the North Central Atlantic Ocean in summer, to the Gulf of Guinea before, during and after each 1st quarter (from Fonteneau et al., 2017).



ICCAT recommendations*: — Rec04 — Rec11 — Rec98, Rec08 and Rec15

*Rec98: Nov. 1999 - Jan. 2004 (FAD)
 Rec04: Nov. 2005 - Nov. 2008 (no-take)
 Rec08: Nov. 2009 - Jan. 2011 (FAD)
 Rec11: Jan. 2012 - Feb. 2016 (FAD)
 Rec15: Jan. 2017 - Feb. 2019 (FAD)

Fig. S10: ICCAT recommendations since their introduction in 1999. FAD stands for fish aggregating devices. (figure from (Stephan et al. 2022)).

Table S1: Summary details of the models used in this application. For each model, the following information is given: number of fixed effects, number of random effects, total estimated parameters and maximum gradient component.

	Fixed	Random	Total	Gradient	Time
GLOBAL	78	47,254	47,332	2.5e – 05	5.22 h
LOCAL	78	20,054	20,132	2.68e – 07	2.05 h

Table S2: Abundance indices per year-quarter

Year	Quarter	Global abundance indices			Local abundance indices		
		Estimate abundance index	SE for estimate	SE for ln(Estimate)	Estimate abundance index	SE for estimate	SE for ln(Estimate)
1993	1	63833	7871	0.146	5886	1295	0.263
1993	2	70754	8622	0.145	4907	1628	0.420
1993	3	56199	8650	0.187	6664	1378	0.245
1993	4	32971	4773	0.173	4328	1110	0.306
1994	1	76478	9919	0.154	5258	1568	0.383
1994	2	78085	10788	0.168	6351	2241	0.467
1994	3	70944	11304	0.197	8704	2619	0.388
1994	4	41987	7055	0.208	4114	1411	0.434
1995	1	66339	9031	0.166	5012	1082	0.257
1995	2	91033	12815	0.174	5181	1786	0.450
1995	3	68856	10194	0.179	5807	1377	0.290
1995	4	37975	6641	0.216	3059	871	0.347
1996	1	75968	9130	0.142	5185	1340	0.322
1996	2	86857	12595	0.176	7773	2262	0.374
1996	3	50522	8175	0.197	6626	1899	0.373
1996	4	36897	6210	0.207	4066	1000	0.302
1997	1	70098	7947	0.131	7213	1651	0.272
1997	2	71943	10141	0.171	10460	3057	0.374
1997	3	55687	10207	0.231	5819	1207	0.246
1997	4	35723	6125	0.210	3717	1349	0.467
1998	1	74665	8662	0.136	3944	837	0.242
1998	2	64471	8607	0.161	6732	1884	0.358
1998	3	55734	9040	0.199	4629	1191	0.323
1998	4	34027	4725	0.163	2127	676	0.396
1999	1	75298	10690	0.173	3960	711	0.202
1999	2	64270	8779	0.165	3635	1311	0.478
1999	3	59432	9595	0.200	3874	1098	0.363
1999	4	30790	4704	0.183	3131	781	0.299
2000	1	55756	6847	0.145	2097	434	0.239
2000	2	59326	10226	0.216	4013	1406	0.466
2000	3	56015	8983	0.196	5882	1206	0.237
2000	4	34701	5579	0.195	2376	603	0.303
2001	1	72405	8570	0.141	4174	1037	0.304

2001	2	83930	11899	0.174	11376	3072	0.347
2001	3	62148	11069	0.222	6396	1462	0.284
2001	4	62252	8401	0.158	5382	1427	0.325
2002	1	86269	9624	0.129	3683	964	0.323
2002	2	73128	10725	0.179	6239	1612	0.319
2002	3	73369	11435	0.191	5261	1590	0.394
2002	4	36612	4896	0.156	2506	686	0.325
2003	1	43819	6131	0.167	2761	637	0.269
2003	2	59261	8587	0.174	5673	1836	0.422
2003	3	47862	7626	0.195	3777	931	0.306
2003	4	29496	4353	0.174	2303	525	0.264
2004	1	52965	6748	0.151	4616	1012	0.253
2004	2	75703	12347	0.201	5438	1534	0.361
2004	3	59763	10686	0.224	5505	1566	0.368
2004	4	39921	6116	0.184	3151	973	0.389
2005	1	48443	6120	0.148	1948	686	0.447
2005	2	53456	8716	0.202	4247	1678	0.526
2005	3	46172	7410	0.196	7283	1744	0.297
2005	4	48696	7201	0.176	2253	755	0.425
2006	1	91182	15057	0.210	2824	830	0.369
2006	2	109322	17910	0.206	6168	2248	0.476
2006	3	80644	13876	0.215	5035	1620	0.420
2006	4	67067	10696	0.195	3148	1218	0.504
2007	1	87965	13758	0.198	1986	583	0.373
2007	2	84800	12731	0.187	2678	992	0.492
2007	3	68331	9969	0.178	2977	878	0.388
2007	4	75158	11185	0.182	2988	832	0.340
2008	1	92815	13219	0.177	10112	2305	0.282
2008	2	92771	13288	0.177	10857	3277	0.399
2008	3	83489	13656	0.206	7188	2087	0.378
2008	4	81996	11639	0.173	4796	1255	0.317
2009	1	71968	10970	0.190	3953	872	0.266
2009	2	69148	9953	0.175	7750	2234	0.372
2009	3	62953	10428	0.205	4912	1219	0.302
2009	4	49272	6842	0.166	3404	1229	0.466
2010	1	53182	6766	0.151	5153	1534	0.385

2010	2	60962	8755	0.175	8125	3138	0.518
2010	3	55091	9255	0.210	6453	1588	0.307
2010	4	46169	6522	0.169	4892	1495	0.385
2011	1	62971	9092	0.179	5447	1564	0.347
2011	2	53630	9316	0.217	6569	2753	0.562
2011	3	44381	7825	0.220	4360	1563	0.468
2011	4	32276	5914	0.228	3863	1486	0.493
2012	1	63944	8483	0.161	4293	1432	0.435
2012	2	53136	7641	0.175	6839	2475	0.481
2012	3	37326	7673	0.264	5421	1324	0.298
2012	4	37206	6186	0.203	3981	1501	0.491
2013	1	59682	9194	0.191	3126	1116	0.473
2013	2	50242	8899	0.222	3728	1378	0.482
2013	3	54757	10052	0.231	4307	1106	0.320
2013	4	36761	6422	0.218	2673	842	0.401
2014	1	59588	8418	0.171	3810	1515	0.531
2014	2	65355	12048	0.238	6081	2632	0.581
2014	3	58524	10435	0.226	4112	1386	0.449
2014	4	58503	9234	0.195	4700	1361	0.357
2015	1	73410	11372	0.192	3875	1087	0.351
2015	2	75155	13483	0.228	7099	2737	0.517
2015	3	72652	14387	0.255	6244	1446	0.289
2015	4	68398	9675	0.173	4283	1363	0.407
2016	1	83291	10886	0.160	2842	1008	0.450
2016	2	78307	14276	0.234	4996	2063	0.554
2016	3	54944	10876	0.253	4809	1202	0.302
2016	4	48569	7703	0.196	2751	1106	0.525
2017	1	70733	10886	0.193	7329	2649	0.478
2017	2	81551	15880	0.255	11101	3538	0.410
2017	3	69952	14098	0.261	11149	3211	0.366
2017	4	60048	8970	0.184	6047	1959	0.411
2018	1	62085	8948	0.177	3270	1134	0.449
2018	2	66090	10790	0.204	6949	2394	0.458
2018	3	52714	9995	0.241	5363	1271	0.284
2018	4	39129	5952	0.186	4333	1390	0.404

References

- Fonteneau A., Alayón P.J.P., Marsac F., 2017, Exploitation of large yellowfin tuna caught in free schools concentrations during the 2013 spawning season (December 2012-May 2013). Collect. Vol. Sci. Pap. ICCAT 73, 868–882.
- ICCAT, 2019, Report for Biennial Period, 2018-2019, Part II – Vol. 2. Standing Committee on Research and Statistics (SCRS). Madrid, Spain 470.
- Stephan P., Gaertner D., Perez I., Guéry L., 2022, Multi-species hotspots detection using self-organizing maps: Simulation and application to purse seine tuna fisheries management. *Methods Ecol. Evol.* 00, 0.